LIMNOLOGY
and
OCEANOGRAPHY

ASLO

Limnol. Oceanogr. 61, 2016, 1574–1588

doi: 10.1002/lno.10297

Influence of ocean circulation changes on the inter-annual variability of American eel larval dispersal

Irina I. Rypina,*[1] Lawrence J. Pratt,[1] M. Susan Lozier[2]
[1]Physical Oceanography Department, Woods Hole Oceanographic Institution, Woods Hole, Massachusetts
[2]Earth and Ocean Sciences, Nicholas School of the Environment, Duke University, Durham, North Carolina

Abstract

American eel (Anguilla rostrata) complete their life cycle by migrating from the east coast of North America to Sargasso Sea, where they spawn planktonic eggs and dye. Larvae that develop from eggs need to return to North American coastal waters within the first year of life and are influenced by the oceanic currents during this journey. A coupled physical–biological model is used to investigate the extent to which inter-annual changes in the ocean circulation affect the success rates of larvae in reaching coastal nursery habitats. Our results suggest that natural oceanic variability can lead to changes in larval success rates by a factor of 2. Interannual variation in success rates are strongly affected by the Gulf Stream inertial overshoot events, with the largest success in years with an inertial overshoot and the smallest in years with a straighter and more southern configuration of the Gulf Stream downstream of Cape Hatteras. The mean Gulf Stream length and latitude between 75W and 70W longitude can be used as proxies for characterizing the overshoot events and can be converted into success rates using linear regression.

The American eel (Anguilla rostrata) is a species of great scientific and economic interest. This catadromous fish, which spawns in the ocean but lives in freshwater throughout most of its life cycle, undertakes a remarkable once-in-a-lifetime migration from its freshwater habitats along the east coast of North America to the Sargasso Sea, where it spawns planktonic eggs and dies (Schmidt 1923, 1925, 1931). Spawning occurs in Feb–Mar of each year, after which eggs hatch into small and vulnerable leptocephalus larvae (McCleave et al. 1987, 1998; McCleave 2008). To develop into juvenile glass eels and then into adults, eel larvae need to reach coastal waters along the North American coast within their first year of life (Kleckner and McCleave 1985; McCleave 1993). Initially, American eel larvae have limited swimming ability; this ability improves in later larval stages (Fisher et al. 2000; Miller 2009) and, after metamorphosing into glass eels, can reach short-term swimming speeds of 11.7–13.3 cm s^{-1} (Wuenschel and Able 2008). Larvae also migrate vertically through the water column from 30–70 m at night to 125–275 m during the day (Castonguay and McCleave 1987), presumably to avoid predators.

Many details of the American eel larvae journey remain a mystery, including the exact location of their spawning site, their ability to navigate by physical cues in the open ocean, their strategy for crossing the strong oceanic transport barriers separating the Sargasso Sea from the coast, namely the Gulf Stream and the continental slope/shelf break front of the Middle- or South- Atlantic Bight, and the extent to which ocean circulation variability can influence variability in the likelihood that larvae will reach coastal nursery habitats. It is the latter mystery that we are trying to clarify in this article.

Specifically, we make use of the coupled physical–biological numerical model developed by Rypina et al. (2014), which combines an eddy resolving model of North Atlantic circulation with a simple but scientifically-motivated swimming and navigation strategy for American eel larvae, to simulate larval migration from the Sargasso Sea to the North American shelf over a 15-yr time interval. Because the biological part of the model is kept unchanged during the entire time interval, the modeled year-to-year changes in larval success in reaching coastal nursery habitats are caused exclusively by variability of the ocean currents. This model experiment allows us to rigorously investigate the influence of ocean circulation changes on larval success rates. We show that success rates are significantly affected by the Gulf Stream and, more specifically, by its geometry just downstream of Cape Hatteras. This link could be potentially

*Correspondence: irypina@whoi.edu

Additional Supporting Information may be found in the online version of this article.

important for fishery and population management as it allows one to infer ocean-circulation-induced variability in larval success rates, which is otherwise very challenging to measure, by monitoring the Gulf Stream using satellite altimetry or other physical oceanographic instruments or models.

Background

Trends and inter-annual variability of the American eel population at various stages of the life cycle

The American eel at various stages of its life cycle from glass eel to yellow and silver eel has long been harvested by both recreational and commercial fishermen, and has an important cultural value for many Native American tribes (Morgan 1877; Speck 1939–1940; Guillet 1957; Tooker 1978). Though these fisheries are seasonal, they provide significant income due to their high price. The commercial harvest of American eel in the USA and Canada exhibits substantial variability (Castonguay et al. 1994; Casselman and Marcogliese 2007; Bonhommeau et al. 2008a,b). The harvest record, which extends back to 1950, shows a pronounced peak around 1975–1980, with a general decline afterwards. The record is also marked by shorter-term year-to-year variations, with harvest values doubling (or halving) in just 1 yr.

Fishery-independent datasets from various surveys and monitoring programs are also available at multiple locations along the North American coast for the yellow eels (YE) and for the young-of-year (YOY) glass eels. In the recent American Eel Benchmark Stock Assessment Report (ASMFC 2012), data from sites sampled for at least 10 yr has been organized into six regions (Gulf of Maine, Southern New England, Hudson Bay, Delaware Bay/Mid-Atlantic Coastal Bays, Chesapeake Bay and South Atlantic) and combined into one dataset for the entire Atlantic Coast. Regional and coast-wide abundance trends, standardized using generalized linear model (GLM) protocols outlined in the Assessment Report Appendix, for both YE and YOY were examined for the presence of multi-year trends and intercompared between different regions. This analysis revealed that while some areas such as Hudson River and South Atlantic showed declines for both YE and YOY, data from other regions showed no significant trends. The long-term (from 1987 to 2009) GLM-standardized abundance index for the YOY along the entire coast varied roughly between 0.9 and 1.7 (in the GLM-standardized units of "numbers caught"; see Fig. 6.2 in ASMFC 2012), but most of this variability lay within, and thus was masked by, large error bars, with only a few years standing out as "extreme good" (1994 with a value of about 1.7 ± 0.25) or "extreme bad" (2000 with a value of 0.9 ± 0.15). Variability is larger for the short-term (2000–2010) abundance index, but so are the error bars, so that trends are again unclear.

Sullivan et al. (2006) made use of two multi-year surveys of ingressing glass eels at two sites—Little Egg Inlet, New Jersey and Beaufort Inlet, North Carolina—to investigate the interannual variability and factors affecting the recruitment of young American eel. Two important conclusions were drawn from that study. First, the interannual variability in glass eel abundance differed significantly between the two sites, without any evidence of synchronicity. Second, the glass eel abundance at each site was significantly positively correlated with local winter precipitation, which was also different between the two locations. The authors hypothesized that glass eels use freshwater signals and salinity gradients as navigational cues for their recruitment into local estuaries. Such a mechanism would explain the mismatches in glass eel abundance at different locations along the North American coast, and would suggest that local variability in glass eel abundance at specific river deltas and inlets may be significantly different from the variability in the total glass eel abundance along the entire coast and, importantly for this study, from the variability in the total larval success rates in reaching the shelfbreak. Note, however, that these same time series, from Little Egg Inlet, New Jersey and Beaufort Inlet, North Carolina, were more recently reanalyzed in the Stock Assessment Report (ASMFC 2012) using the GLM-standardized abundance index approach. That analysis revealed a significantly larger degree of temporal synchronicity between the two sites than found by Sullivan et al. (2006).

Many factors influencing the population levels of the American eel could contribute to the observed variability at various stages of the fish life cycle, including overfishing, anthropogenic changes to the natural habitats, the effects of regulatory eel fishing limits, variations in food availability, and changes in the oceanic circulation. Different factors act during different stages of the American eel life cycle. Specifically, anthropogenic changes such as river damming would directly affect the continental phase of the life cycle including stages from elvers to YE, whereas changes in the open ocean circulation would directly influence the oceanic phases of the life cycle (i.e., silver eels, eggs, larvae, and glass eels) that bookend the continental phase. However, because each successful individual needs to go through all of the life stages, the direct effects acting on one particular life stage would indirectly affect all of the subsequent life stages. For example, the total abundance of the YOY American eels along the entire coast in a given year depends directly on ocean circulation changes, but it also depends on the number of eggs spawned during that year, which itself depends on the number of silver eels that successfully migrated to the Sargasso Sea that year, which in turn depends on various factors affecting the population of the YE during the preceding years.

The interplay between the various factors described above makes it extremely challenging to predict or even interpret the observed trends in the eel population variability.

Comparisons between observed trends and numerical models of the American eel population are also difficult because a realistic model needs to represent all stages of the eel life cycle, and correctly predict the response to changes in the various factors affecting the eel population at each stage, as well as correctly account for the multi-faceted interactions between different life stages. In this article, we focus on a much simpler and narrower task. Using a coupled physical–biological modeling framework, we investigate whether and to what extent interannual variability in the open ocean circulation can directly affect the success rates of American eel larvae in reaching North American coastal areas. Our work focuses on the variability that occurs during the larval stage as a result of changes in the ocean circulation. Since we do not take into account other factors and other stages of the American eel life cycle, any comparison with observed trends in the total commercial harvest or YOY abundance indexes needs to be interpreted with care. Nevertheless, our approach provides a systematic way to rigorously quantify the limits of variability for at least one aspect of this complicated problem.

Swimming and navigation strategies of American eel larvae

The swimming and navigation strategy of American eel larvae is poorly known. Recently, Rypina et al. (2014) used a coupled physical–biological model to investigate how different behavioral adaptations and navigation strategies influence the ability of American eel larvae to reach near-coastal waters. In that paper, the authors tested 4 different swimming and navigation scenarios—passive drift, random walk swimming, and directional navigation with and without a preferred swimming direction. They found that the ability of American eel larvae to swim and maintain direction is crucial for reproducing a reasonable distribution of larvae along the North American east coast. Other swimming strategies, such as passive drift (i.e., larvae are passively advected by oceanic currents) or random-walk-like swimming (i.e., larvae can swim horizontally but change direction randomly during their journey), led to large spatial gaps along the North American coast and an absence of simulated larvae along the Gulf of Maine, where juvenile eels are harvested each year, and the east coast of Canada. Note that the only available data for recruitment is for glass eels in select inshore areas: no data on larval recruitment exists at the shelf break. In the same paper, the authors investigated larval success rates with respect to larval swimming direction. They found that the dependence on swimming direction was approximately Gaussian, with the optimal swimming direction to the northeast from the Sargasso Sea, a direction that is mostly independent of the larval swimming speed. The total larval success rates were 3.5 times larger for the directional swimming strategy with the preferred optimal direction compared to simulations without a preferred direction. It has been hypothesized in prior literature (Kleckner and McCleave 1985; Miller 2009; Righton et al. 2012) that American eel larvae have developed a genetic memory and evolved to orient in a particular direction to optimize their chance of survival. Simulations from Rypina et al. (2014) strongly suggest that such an optimal direction would be at a compass heading of 300°, i.e., to the northwest from Sargasso Sea.

Directional navigation, such as the one hypothesized in Kleckner and McCleave (1985), Miller (2009), and Righton et al. (2012), implies the ability of larvae to maintain their heading using some physical, chemical or other cues. Several potential cues have been proposed and discussed in the literature, including hearing and olfaction (Atema et al. 2002; Montgomery et al. 2006), gradients in the physical characteristics of the seawater such as temperature or salinity (Sullivan et al. 2006), navigation using bathymetry, oceanic currents, sunlight, celestial bodies, polarized light, or geomagnetism (Mouritsen et al. 2013). Some of these strategies, specifically hearing and olfaction and gradients in salinity or temperature, seem to be better suited for the small-scale near-shore environments where sound sources are more local, sounds are louder and gradients of water properties are larger, rather than for navigation in the large-scale open ocean where gradients are much weaker. Thus, to navigate by chemical gradients in the open ocean, slow-swimming larvae would need to "remember" conditions that occurred perhaps days to weeks prior. Navigation using bathymetry is also unlikely as larvae stay too shallow to see or feel any bottom effects in the open ocean, and navigation by sunlight is improbable because larvae migrate downward during day time, which would make it very challenging to detect the angle of the sun. Sensing oceanic currents would also be challenging as the slow-swimming larvae stay entrained in a parcel of water and thus are unlikely to be able to feel their ground speed. Perhaps the most promising cue that American eel larvae could use in order to orient in the open ocean is geomagnetism. In support of this strategy, recent experiments by Durif et al. (2013) have suggested that adult eels can orient in accordance with magnetic fields. Several other studies have suggested that larvae of several other fish species could use geomagnetism to orient and swim directionally (Wiltschko and Wiltschko 1995; Lohmann et al. 2007; Mouritsen et al. 2013). We know of no studies that detect or measure this ability in American or European eel larvae.

Influence of the Gulf Stream on larval species

The dynamic and energetic Gulf Stream (GS) system with its extension, meanders, warm- and cold-core rings and streamers has been known for decades to influence the spatial distributions of larvae for several fish and invertebrate species that spawn both in the inner and outer parts of the continental shelf, as well as in the Gulf of Mexico. This list includes bluefin tuna, bluefish, blue crab, Atlantic menhaden, mullets, and several species of sciaenids (e.g., weakfish,

croaker, red drum), flounders, and other groundfish. For example, McGowan and Richards (1989) suggested that GS advection was responsible for the presence of larvae of bluefin tuna, which spawn in the Gulf of Mexico, as far north as Cape Fear, North Carolina. Hare and Cowen (1996) showed that larvae of bluefish, which spawn near the outer edge of the shelf in the South Atlantic Bight, are entrained into the western edge of the GS, transported northward and then entrained into warm-core rings that bring the late-stage larvae to the shelf edge of the Mid-Atlantic Bight where they recruit as juveniles into estuaries (see also Hare and Cowen 1991; Cowen et al. 1993; Hare and Cowen 1996; Hare et al. 2002). Two other species of great importance, whose larval distributions are likely influenced by the GS system, are blue crab (Goodrich et al. 1989; Epifanio 1995; Garvine et al. 1997; Etherington and Eggleston 2003; McMillen-Jackson and Bert 2004; Tilburg et al. 2007) and Atlantic menhaden (Checkley et al. 1988, 1999; Govoni and Spach 1999; Hare et al. 1999; Quinlan et al. 1999; Stegmann et al. 1999; Werner et al. 1999; Lozano et al. 2012; Lozano and Houde 2013). The American Eel, which is the focus of this study, differs from the above-mentioned species in two aspects: the far-offshore location of the spawning ground (Sargasso Sea vs. coastal regions for other species) and the much longer duration of the larval phase (1 yr vs. several weeks). Because of the first difference, the strong dynamic constraint placed on cross-stream transport will play a critical role in the success of American Eel larvae.

Methods: Coupled physical–biological model for American eel larval dispersal

In this article, we take advantage of the physical–biological modeling framework developed in Rypina et al. (2014) to simulate the dispersal of larvae from the Sargasso Sea. The ocean currents in our model are produced by the Family of Linked Atlantic Model Experiments (FLAME) ocean general circulation model (Boning et al. 2006; Biastoch et al. 2008), which was configured to cover the entire North Atlantic basin over 1990–2004 with 1/12° horizontal resolution and 45 z-coordinate vertical levels. Note that the results in Rypina et al. (2014) were based on a 5-yr segment of the same model run, whereas the present analysis is based on a full 14 yr. After a 10-yr spin-up, monthly averaged flux anomalies from the National Centers for Environmental Prediction and National Center for Atmospheric Research were superposed on European Center for Medium-Range Weather Forecasts monthly flux climatology and used as surfacing forcing. The model output was saved every 3 d. The model is eddy permitting, exhibits realistic time-averaged and eddy fields, and has previously been used for studies in the Gulf Stream/Sargasso Sea domain in Rypina et al. (2014), Burkholder and Lozier (2011, 2014), Gary et al. (2014) and Kwon et al. (2015). However, the model's spatio-temporal resolution and its absence of freshwater coastal sources and tides lead to less reliable spatial and temporal patterns for the coastal ocean currents. As in Rypina et al. (2014), we therefore focus on the larval transport from the Sargasso Sea to the 200 m isobath—a demarcation considered to be the off-shore edge of the shelfbreak—rather than all the way to the coast. Larvae able to cross the 200 m isobath will be referred to as successful larvae in the remainder of this article.

The diel vertical migration of eel larvae is simulated by constructing effective night-time and day-time oceanic velocities: horizontal currents at each grid are averaged between 25 m and 76 m at night and between 124 m and 290 m during the day and then used to advect simulated larvae. Larvae in our model develop better swimming ability as they mature. This ability is implemented as a linear increase in their swimming speed from 0 at time of release to 6 cm s^{-1} after 1 yr. The latter speed has been estimated as the average long-term swimming speed of glass eels (Wuenschel and Able 2008). Active horizontal navigation is implemented by assigning simulated larvae a preferred northwestern swimming direction according to a Gaussian distribution of angles with mean and std values as in Rypina et al. (2014) (their scenario 4). These active swimming velocities are superposed on the effective day-/night-time oceanic currents, and this total velocity is used for the computation of larvae trajectories using the variable-step Runge-Kutta method (RK45 in MATLAB) with bi-linear interpolation in space and time between the grid points. Similar to Rypina et al. (2014), simulated larvae are released every week during the 3-month spawning season from February to April each year in the rectangular domain (74W to 55W and 22N to 30N) covering the Sargasso Sea, and their trajectories are calculated over 1 yr from release. One million simulated larval particles are released each year. Larval mortality is implemented through the exponential decay of surviving larvae at a rate of 3.8 per year, which leads to a larval population after 1 yr that is just 2% of its original size (Bonhommeau et al. 2009; Rypina et al. 2014).

In the next section, we use this coupled physical–biological model to simulate larval success rates from 1990 until 2003, and we identify factors in the oceanic circulation that have the major influence on larval success in our model. We find that the behavior of the Gulf Stream just past the separation point where it detaches from the coast at Cape Hatteras plays a critical role in the ability of larvae to reach the coastal areas, and we develop two relevant Gulf Stream (GS) indices: the mean GS length and the mean GS latitude averaged between 75W and 70W. It is important to note that we do not expect the inter-annual variability of the Gulf Stream simulated by FLAME (or any other nondata-assimilative model) to have contemporaneous agreement with the observed interannual variability of the Gulf Stream. Instead, we rely on FLAME to suggest physical mechanisms, and their

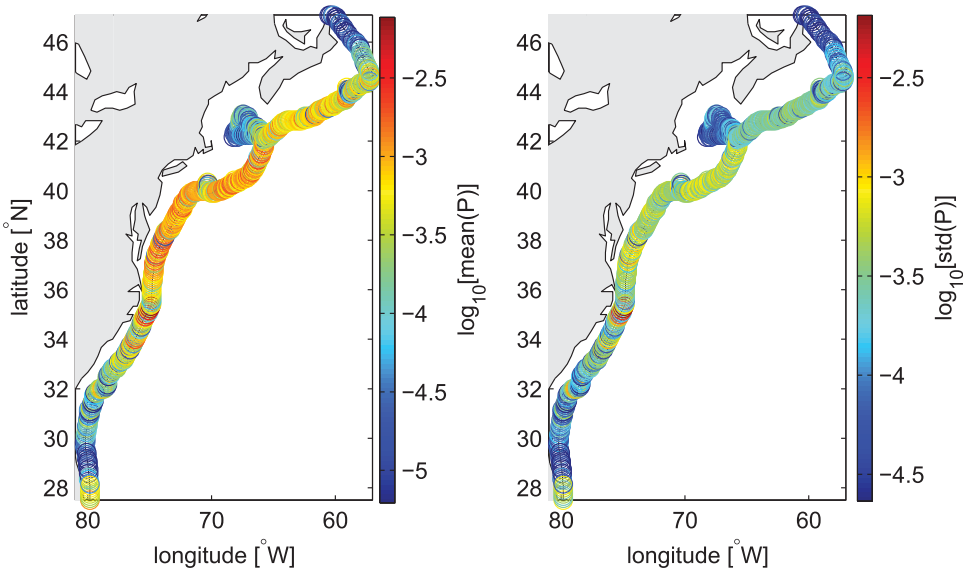

Fig. 1. Mean (left) and std (right) of modeled larval success rates along the 200 m isobath. Success rates (in %) are shown on a logarithmic color scale.

proxies, contributing to variability, especially those mechanisms associated with crossing the GS. To do so, we must have confidence that FLAME adequately simulates the envelope of expected variability, an issue explored in detail in "Inter-annual variability in larval success inferred from satellite altimetry" section. We find a favorable comparison between model-based indices and those based on observed satellite altimetry. Given this comparison, we assess and quantify the impact of ocean-induced changes on the temporal variability of larval success rates in our model and in the real ocean. Our results are summarized and discussed in the final section.

Results

Inter-annual variability of larval success rates

Ingressing glass eels enter rivers and estuaries along the North American coast from the tip of Florida Keys to Hudson Bay each year (ASMFC 2012, 2014). Consistent with this observation, the spatial distribution of larval success rates in our model (Fig. 1a) shows nonzero probabilities along the entire North American coast. Both larval success (Fig. 1a) and its variability (Fig. 1b) are spatially nonuniform, with elevated values over the Mid-Atlantic Bight between Cape Hatteras and Gulf of Maine (Fig. 1).

Our coupled physical–biological numerical model of American eel larval dispersal suggests significant inter-annual variability in these larval success rates (Fig. 2). Over our temporal interval of 1990–2003, larval success rates reach a maximum of 0.47% in 1994 and a global minimum of 0.22% in 1999. Variations between two consecutive years are smaller but still significant, with the largest change observed from 2002 (0.3%) to 2003 (0.46%). As the biological component of the

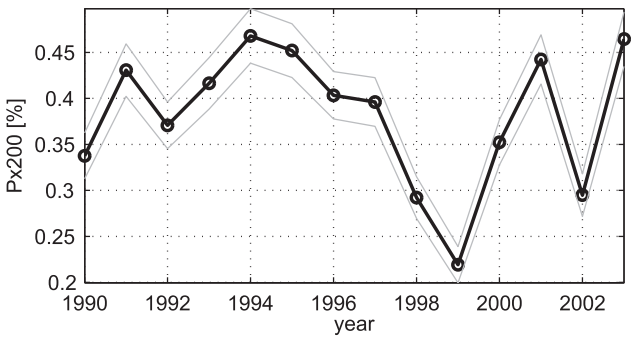

Fig. 2. Time series of the success rates for larvae reaching the 200 m isobath. The gray lines mark the 2-std interval around the mean (black). Standard deviations for each year were computed via a bootstrap method using 500 randomly drawn ensembles of 1 million simulated larvae.

model (i.e., the horizontal swimming strategy, vertical migration and mortality) is held constant for all years, we attribute this variability in larval success rates to changes in the ocean circulation. We next focus on the specific changes in the ocean circulation that have the key effect on larval success rates. Specifically, we investigate the influence of the shape and strength of the GS where it leaves the coast, the mean and kinetic energy of the GS and the overall effect of eddies. Each of these mechanisms is discussed in turn in this section.

The shape of the Gulf Stream and "inertial overshoot" events

The Gulf Stream is directed northward along the North American coast from the tip of Florida until about Cape Hatteras, where it separates from the coast and flows

northeastward into the open ocean. As a water parcel or an organism tries to cross the Gulf Stream, it is swept downstream by the strong current and eventually diverted offshore. Thus, the Gulf Stream presents a serious obstacle for larvae trying to reach coastal waters. A recent study has documented that this barrier strongly influences larval success rates (Rypina et al. 2014), a result consistent with other studies focused on the movement of floats or drifters across this current (Bower and Rossby 1989; Bower and Lozier 1994; Brambilla and Talley 2006; Burkholder and Lozier 2011; Rypina et al. 2011).

Past its separation point at Cape Hatteras, the Gulf Stream is unstable and exhibits characteristic meanders. These meanders can at times be of sufficient amplitude such that they detach, forming warm- and cold-core eddies that travel westward toward the coast. These meanders and eddies facilitate cross-stream exchange, thus increasing the chances that an organism will cross the Gulf Stream and reach coastal areas. Interestingly, the location of the Gulf Stream's separation from the coast can vary. Though it is on average near Cape Hatteras, it sometimes "overshoots" this usual separation location, detaching instead slightly further north. This well-documented behavior is often referred to as the "inertial overshoot" of the Gulf Stream (Dengg 1993; Dengg et al. 1996; Özgökman et al. 1997; Zhang and Vallis 2007; Pierini et al. 2011).

The influence of the GS on larval success rates in our biophysical model was examined by computing a sequence of probability maps showing where and with what probability successful larvae cross the north wall of the GS during each year (Fig. 3). We define the instantaneous position of the GS north wall as a function of longitude in each 3-d snapshot of the model's temperature field as the location where the 15°C isotherm intersects 200 m; this standard definition has been used in the literature for decades (Fuglister 1955). We then count how many successful simulated larvae cross that instantaneous north wall at different longitudes. Because the GS shifts and meanders as the flow evolves with time, the resulting probability maps show nonzero values within the envelope of instantaneous GS positions for each year, with the envelope itself also changing from year to year (2 bottom rows of Fig. 3). After inspecting all 14 yr, we picked the years with the largest (1994), smallest (1999) and intermediate (1990) larval success rates for closer study (top row of Fig. 3). The major differences between these three probability maps appear just downstream of Cape Hatteras. Specifically, in 1999 (Fig. 3 top right panel), which is the year with the smallest larval success rates, the GS separated from the coast at Cape Hatteras (36N) and flowed offshore in an almost straight configuration without meanders. In contrast, in 1994, the year with the largest larval success rates, the GS followed the coastline much further north and separated from the coast at around 40N, exhibiting a strong inertial overshoot. Finally, in 1990, which is the year with intermediate larval success rates, the GS was in an intermediate state of weak inertial overshoot, where it separated from the coast at around 37N.

A qualitative comparison among these 3 yr suggests that the probabilities and locations where successful larvae cross the GS are significantly affected by the inertial overshoot. This suggestion is quantitatively confirmed in Fig. 4, where the percentage of successful larvae crossing the GS at different longitudes is shown. Gray curves in Fig. 4 correspond to individual years, and were created by summing the probabilities shown in Fig. 3 over all latitudes (i.e., collapsing the map onto a longitudinal axis). As seen in Fig. 4, the largest year-to-year variations in the percentage of successful larvae crossing the GS occur between 70W and 75W, which is the area of the inertial overshooting. Note that the large values of success rate between 80W and 78W in Fig. 4 are due to the fact that much of the coastline south of Cape Hatteras is squeezed into this longitude band.

To understand the relative importance of the 70W and 75W longitude band as a function of time, we have split the total larval success rate (black curve in Fig. 5) into contributions from different longitudinal bands (marked with different colors in Fig. 5). Consistent with Figs. 3, 4, the longitudinal band between 70W and 75W is a region of strong exchange, accounting for 40–50% of the total larval success each year. The red and black curves in Fig. 5 are strongly correlated ($r = 0.75$), confirming that much of the interannual variability in the total larval success comes from the area of inertial overshoot.

Proxies for inertial overshoot events

It is evident from Fig. 3 that the inertial overshoot events are characterized by a northward shift in the GS separation from the coast and by an increase in the arclength of the GS downstream of Cape Hatteras, which leads to a longer jet centerline between 70W and 75W. Thus, to quantitatively examine the impact of overshoot events on larvae success rates, we use the mean GS latitude and mean GS arclength, spatially-averaged over the geographical area of inertial overshoot (70W and 75W), as proxies for the overshooting. These proxies are compared to larvae success rates for each year in the upper two panels of Fig. 6. Consistent with the shape of the GS depicted in the lower panels of Fig. 3, both the mean GS latitude and length indicate that in 1991 and from 1994 to 1997, the GS had a longer jet centerline and it was located further north, while in 1998–2000 it had a straighter, shorter and more southern configuration. Thus, the former/latter time period was characterized by strong/no inertial overshoot. As expected, the two proxies (black curves in Fig. 6 top panels) are strongly correlated with each other ($r = 0.94$) and each has a strong correlation ($r \backsimeq 0.9$) with larvae success rates (P_{75to70}) within the inertial overshoot longitudinal band (red curves in Fig. 6). The correlation of these proxies with the total larval success (not shown) is also significant, with a correlation coefficient of $\backsimeq 0.6$ for both proxies.

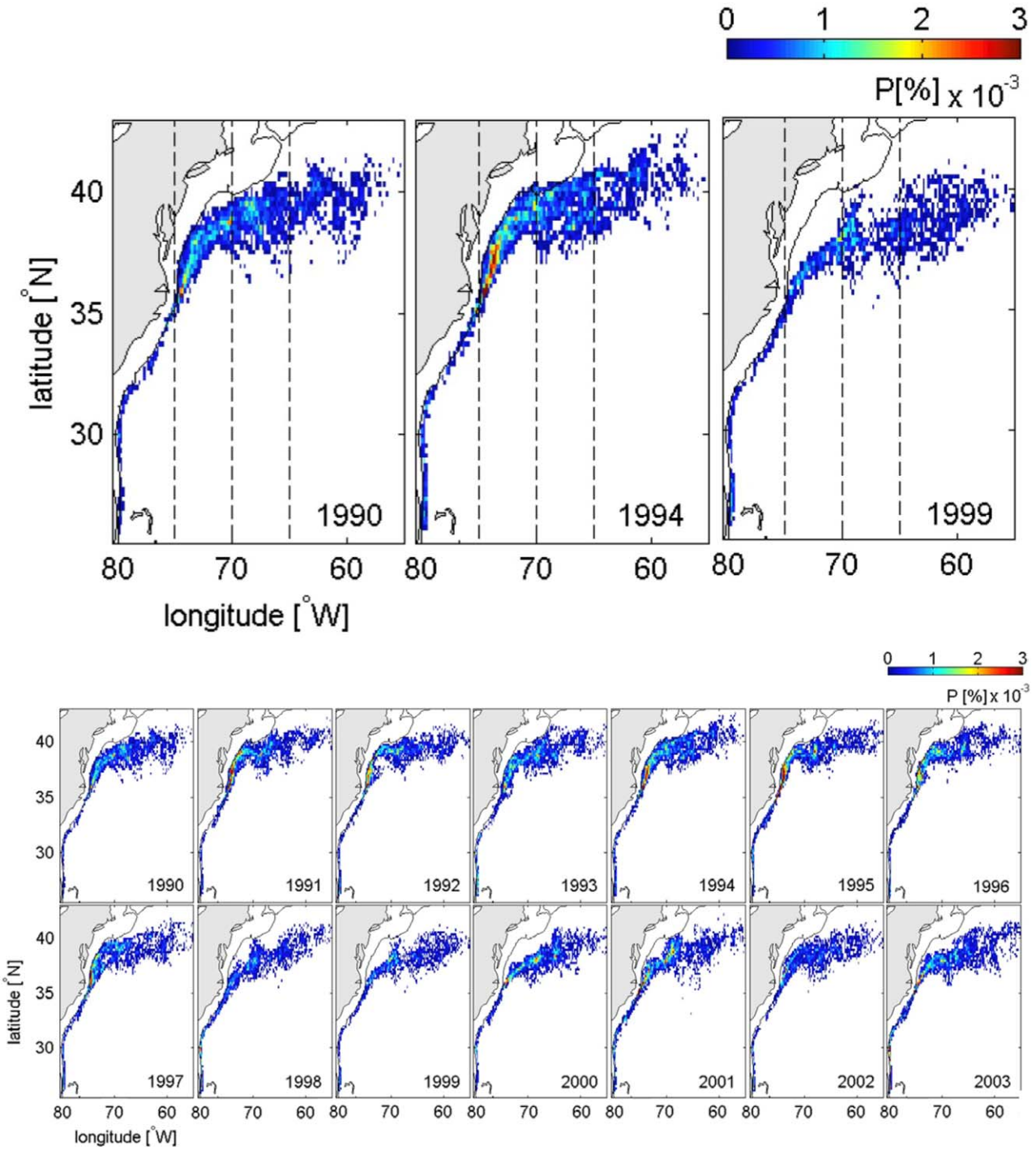

Fig. 3. Probability map showing where successful larvae cross the Gulf Stream in different years. Color indicates percentage of larvae crossing the Gulf Stream at a given location.

Impact of GS mean and eddy kinetic energy on larval success rates

We next examine whether there is a relationship between larval success rates and the strength of the Gulf Stream current between 70W and 75W, as measured by its mean and eddy kinetic energy. A stronger mean current (larger mean kinetic energy) is expected to inhibit cross-stream larval transport and thus decrease the larval success since a stronger current is more likely to move the particles downstream, away from the coast, before they have a chance to cross the current. Also of note is

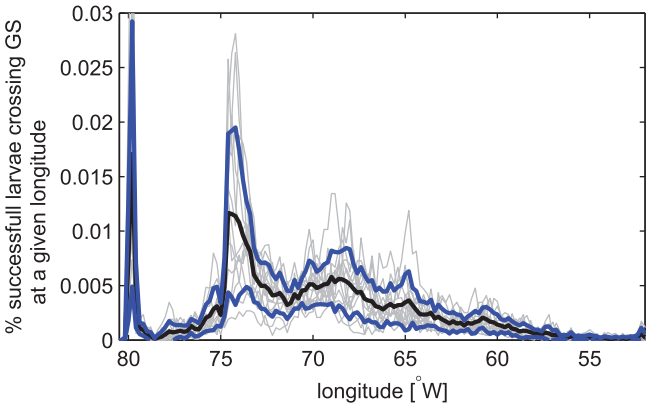

Fig. 4. Percent of successful larvae crossing GS at a given longitude. Gray shows individual years; blue shows a 1-std interval around the mean (black).

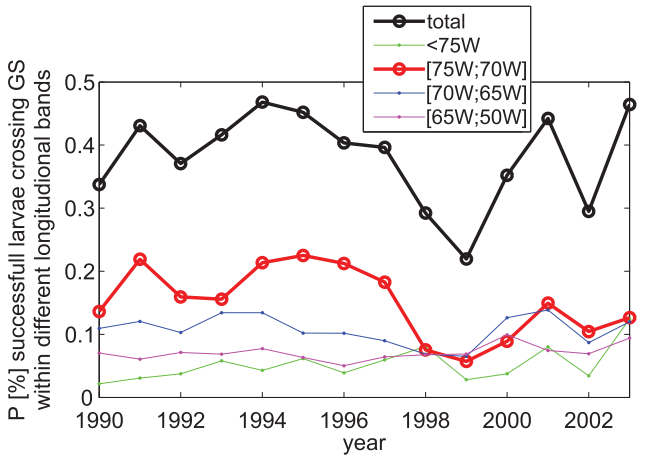

Fig. 5. Percent of successful larvae crossing GS within different longitudinal bands.

that the overshoot events are essentially large-scale meanders of the GS. Thus, these events are expected to be characterized by an increase in the eddy kinetic energy and a decrease in the mean kinetic energy. A straight and more southern configuration of the GS would be characterized by relatively low eddy kinetic energy and high mean kinetic energy. Consistent with this expectation, the eddy/mean KE (black curves in the bottom panels in Fig. 6) show a pronounced minimum/maximum during 1998–2000 (years with the straightest and southernmost GS and no overshoot), when larval transport is at its minimum. However, agreement in other years is less clear, with the correlation between eddy/mean KE and P_{75to70} (0.57 and −0.62, respectively) significantly smaller than the correlations between P_{75to70} and GS length and latitude.

A model for reconstructing larval success rates from mean GS length and latitude

There is a clear relationship in our physical–biological model between GS inertial overshoot events and larval success rates, with increased larval success during overshoot years. The relationship between the strength of the GS, as measured by the mean kinetic energy, and larval success is, on the other hand, not conclusive.

Given the success of the proxies for overshoot events, specifically, mean GS latitude and length within the inertial overshoot longitudinal band, we introduce a simple analytical model for reconstructing larval success rates from the proxies. Such a model would allow us to take what we have learned from FLAME to see what larval success rates might be based on the observed GS length and latitude from satellite altimetry or other measurements. A simple model of this type could be constructed based on a linear regression, $P_{reconstructed}$ [in %] $= a \times$ (GS length [in km] or latitude [in °N]) $+ b$.

Before applying this formula to the satellite-based GS proxies, we test its performance using FLAME-based model. The reconstructed time series of larval success rates, both for the total percent of successful larvae, P_{tot}, and the percent of successful larvae crossing the GS between 75W and 70W, P_{75to70}, are shown in Fig. 7. The reconstructed time series for P_{75to70} (dashed and dotted pink curves) agree well with the "true" time series (solid red curve). This agreement is not surprising given the high correlation between the proxies and P_{75to70}. The agreement between the reconstructed time series (dashed and dotted gray curves) and P_{tot} (solid black curve) is reasonably good from 1990 until 1998 but worsens over the last 5 yr of the simulation (1999 to 2003). Figure 5 suggests that the reason for this disagreement could be related to the relatively larger contribution of the longitudinal bands other than the one that contains the inertial overshoot to the total larval success rates (black curve in Fig. 5), specifically the 65–70W and to a lesser degree < 75W (blue and green in Fig. 5) bands. Thus, although well-captured by the proxies, the variability within the overshoot band alone cannot fully reproduce the variability of the total success rates during this time period. However, the mean relative error (i.e., mean(abs(P_reconstructed-P))) for the reconstructed larval success rates is only ∼ 15% for both P_{tot} and P_{75to70} owing to the larger mean value of P_{tot}. On the other hand, the fraction of variability captured by the reconstructed time series is significantly larger for P_{75to70} than for P_{tot} ($r^2 \sim$ 80% and $r^2 \sim$ 40%, respectively). Note that the described reconstruction formula is based on a simple single-variable linear regression; a more sophisticated multivariate and/or non-linear model might yield better results.

Importance of eddies

The large interannual variability of larval success rates in our model points to the importance of the eddying component of the oceanic flow field. The strong effect of the GS inertial overshoot events on larval success rates is consistent with this general expectation. However, the inertial overshooting of the GS is just one manifestation of a strongly-

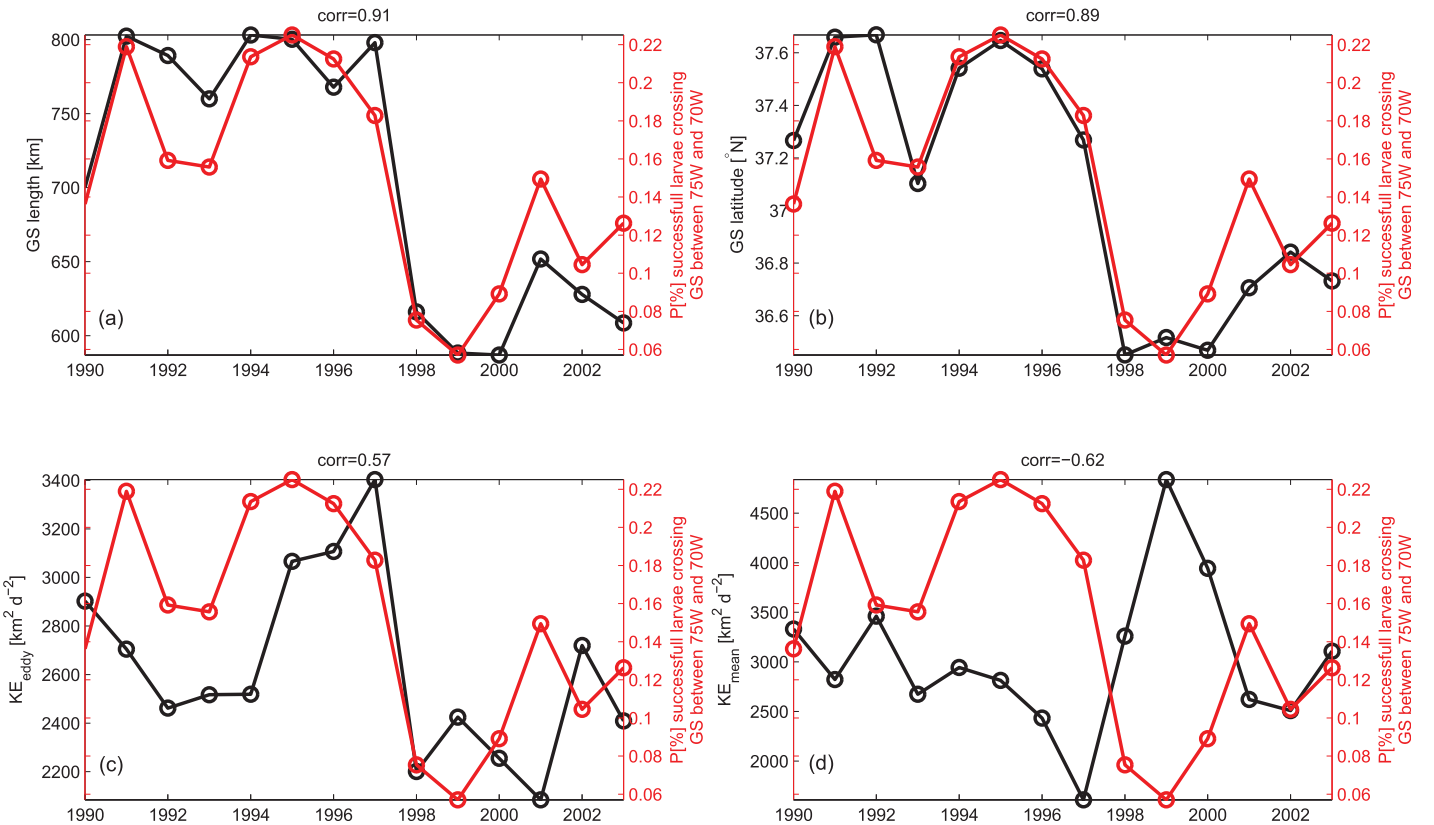

Fig. 6. GS length (a), mean GS latitude (b), eddy KE energy in the GS region (c), and mean KE in the GS regions (d) computed between 75W and 70W and averaged in time from August of the release year (when larvae released in the Sargasso Sea start to reach the GS Extension region) to April of the next year (black). Red curve is as in Fig. 5. Correlation between black and red curves is shown above each subplot.

varying flow field. Other examples include flow instabilities, propagating vortices, rings or coherent eddies, spontaneous squirts and jets that occur in response to local or remote forcing events, as well as more systematic seasonal changes and interannual variations of the oceanic currents. Investigating and quantifying each of these effects separately would be quite challenging. However, their collective impact can be easily quantified by defining the eddy field in the most general sense as the time-varying component of the flow that includes everything but the mean. Removing this eddy field from the total FLAME-based velocities and then re-calculating larval success rates yields a measure of the eddies' contribution to these rates. As seen in Fig. 8 the removal of eddies has a strong effect on both larval success rates and larval travel times, with the success rate decreasing by a factor of 3.4 and the travel times at many locations increasing from well under 1 yr to over 1 yr. Recall that the duration of the larval phase for American eel larvae is about 1 yr, so travel times exceeding this value are unrealistic from the biological perspective. Thus, eddies not only significantly aid larvae in reaching the 200m isobath, but also keep larval travel time within the limits dictated by American eel biology.

Inter-annual variability in larval success inferred from satellite altimetry

The ability of ocean circulation models to faithfully reproduce the ocean's velocity and property fields depends upon many factors, including resolution, parameterizations, approximations made to the Navier-Stokes equations, an incomplete set of forcing mechanisms, the imposition of imperfect initial and boundary conditions etc. Thus, without data-assimilation, it is challenging to replicate the state of the real ocean at any given time. Instead, an ocean circulation model is expected to reliably reproduce the type of features known to exist in the real ocean, as well as their spatio-temporal statistics and energy characteristics. For example, instead of replicating the exact shape of the GS with all its meanders and eddies at any given time, the model should produce a realistic realization of the GS, that would, on average, produce meanders and rings of the same size, duration and energy distribution as in the real ocean. A similar argument applies for the inertial overshoot events: FLAME is not designed to reproduce each specific overshoot event, rather it is expected to produce realistic inertial overshoot events of comparable magnitude and duration as those in the real ocean. If these expectations are met, we are

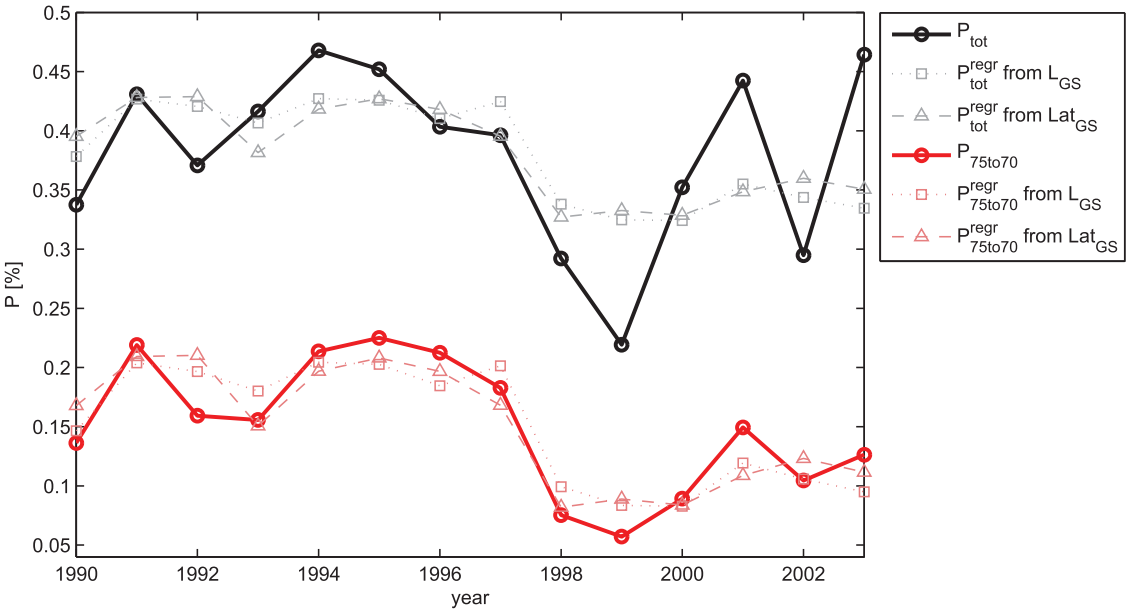

Fig. 7. For the coupled physical–biological model, true (solid) and reconstructed (dashed and dotted) larval success rates obtained from the mean GS length and latitude using the linear regression method. Black shows total % of successful larvae; red shows % of successful larvae crossing GS within the 75W to 70W overshoot longitudinal band. The estimated values for the dimensional coefficients in the linear regression formula, $P_{\text{reconstructed}}$ [in %] = a*(GS length [in km] or latitude [in deg N]) + b, are $\{a, b\} = \{5.127 \times 10^{-4}, 2.645 \times 10^{-3}\}$ for the GS length and $\{9.202 \times 10^{-2}, -3.049\}$ for GS latitude regressions to the total success rate; and $\{a, b\} = \{5.623 \times 10^{-4}, -0.247\}$ for the GS length and $\{0.105, -3.761\}$ for GS latitude regressions to the success rate within the overshoot band.

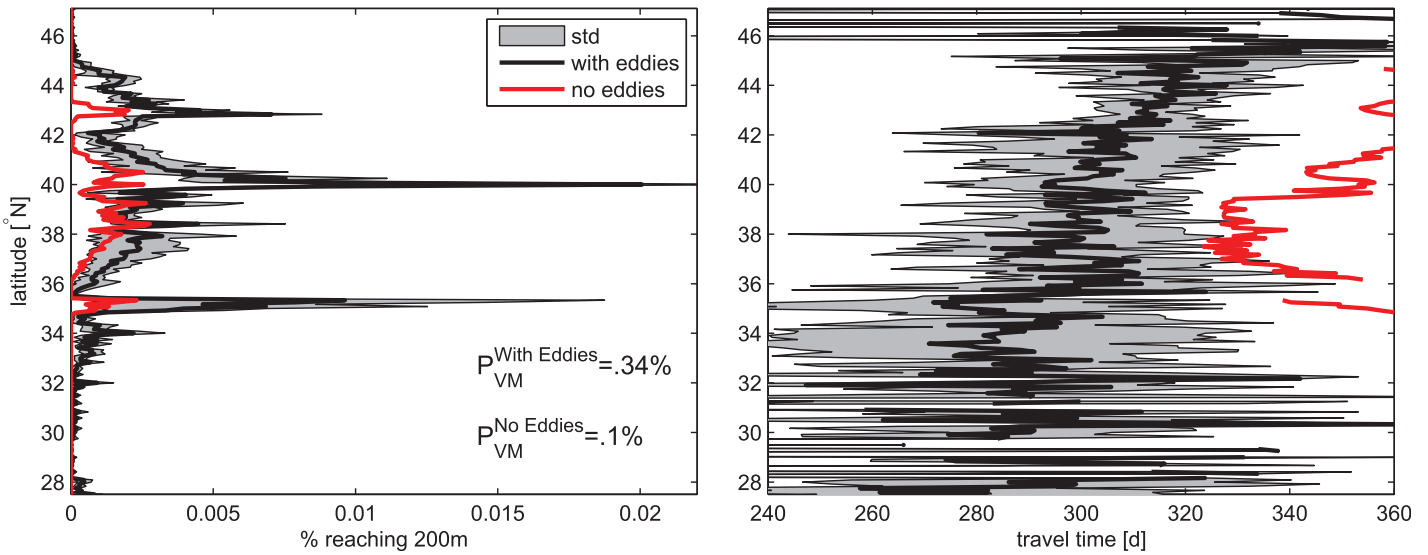

Fig. 8. Success rate (left) and travel time (right) of larvae as a function of latitude in simulations where larvae are advected by the total velocity field (mean + eddies − black) and by the mean velocities only (no eddies—red). Grey indicates the 1-std interval around the mean. Numbers in the left subplot indicate larval success rate in both simulations.

comfortable using the model to explore the relationship between inertial overshoots and larval success rates.

The comparison between mean GS length and latitude (our proxies for characterizing inertial overshoot events) computed using FLAME-based velocities and mean GS length and latitude computed using AVISO-based geostrophic currents is shown in Fig. 9. Because FLAME does not assimilate data, it does not reproduce the observed temporal evolution of the AVISO-based fields. However, as stated above, such direct agreement between the two is not required for our

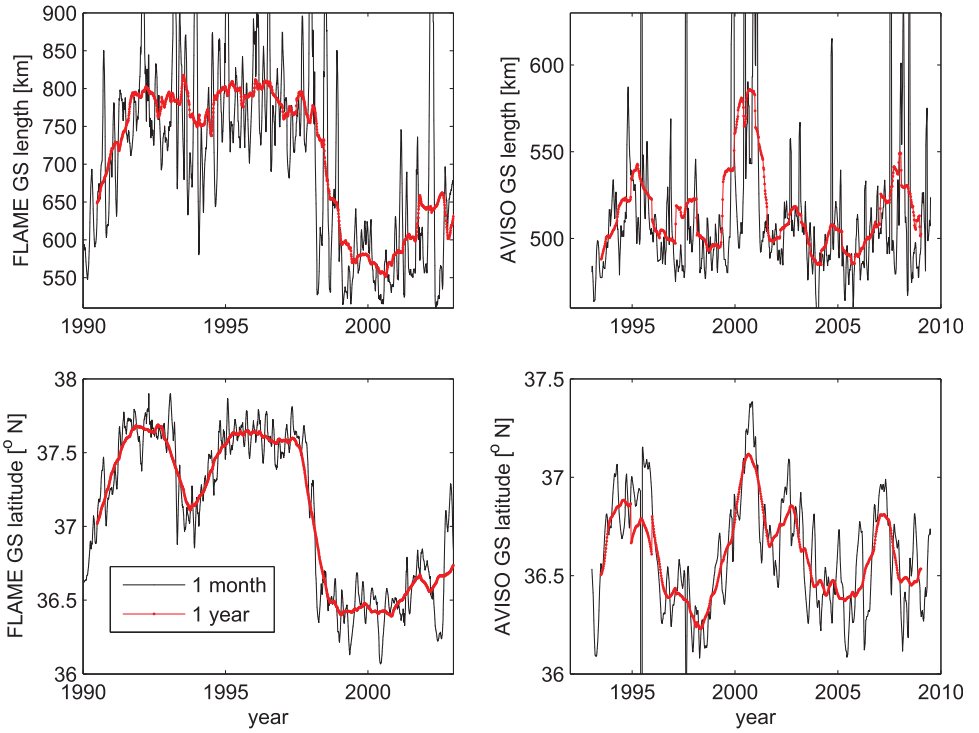

Fig. 9. For the FLAME model (left) and for the SSH-based AVISO velocity fields (right), GS length (top) and mean latitude (bottom) between 75W and 70W, computed with1 month (black) and 1 yr (red) temporal running-averaging.

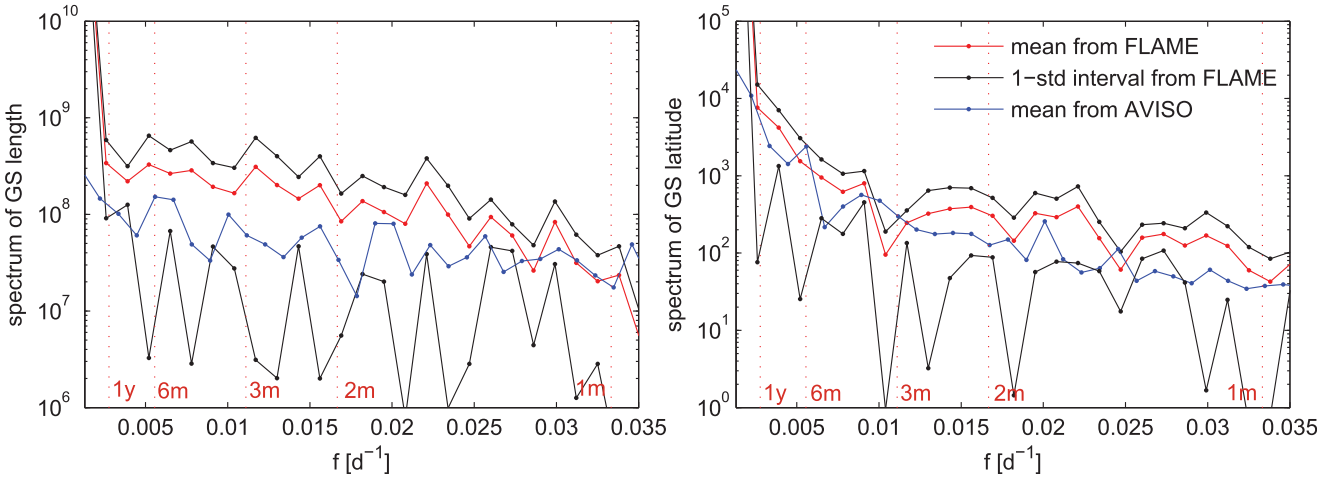

Fig. 10. Power spectra of the time series of the mean GS length (left) and GS latitude (right) between 75W and 70W for FLAME and AVISO. Mean and 1-std interval for FLAME, obtained by splitting the time series into non-overlapping 3-year-long segments, are shown by red and black; mean for AVISO is shown in blue. For reference, red dotted vertical lines mark periods from 1 month to 1 yr.

purposes. Instead, we compare the magnitude of variability (Fig. 9) and the frequency content (Fig. 10) of the FLAME and AVISO time-series for the mean GS length (top) and latitude (bottom) to assess if they are statistically similar. For both FLAME and AVISO, the two proxies show good agreement (correlation coefficient between the red curves on the top and bottom panels of Fig. 9 is 0.66 for AVISO and 0.67 for FLAME), with length being noisier than latitude in both cases. The magnitude of variability is comparable but slightly smaller for the AVISO fields, with GS length varying from 460 km to 580 km (vs. 600 km to 800 km for FLAME) and GS latitude varying from 36.25N to 37.1N (vs. 36.6N to 37.6N for FLAME). The frequency content for both time series is shown in Fig. 10. For each time series, the mean

spectrum was computed by splitting the entire available time-series into nonoverlapping 3-yr segments, and then averaging the resulting spectral amplitudes at each frequency. The result suggests that the mean spectra produced from the AVISO time-series for both GS length and GS latitude lie within the 1-std interval of the corresponding FLAME-based spectral estimates for a wide range of frequencies from 1 month to over 1 yr. Note that due to the splitting of the time-series into shorter segments, the long-term variability is poorly resolved in the resulting spectra.

Using the linear regression formula introduced at the end of subsection "A model for reconstructing larval success rates from mean GS length and latitude" with the linear regression coefficients (from the caption of Fig. 7) inferred from FLAME-based coupled model, AVISO-based mean GS length and latitude can be easily converted into a time series for larval success rate, leading to interannual variations in the larval success rates of approximately 30% compared to the mean values. Note, however, that based on the FLAME model, the reconstructed variability accounts for only about 40% of the true variability, suggesting that the observed AVISO-based oceanic variability can cause inter-annual variations of 75% in larval success rates.

A number of parameter values were assigned within our bio-physical model, and many, if not all, are not very well-known and have large uncertainties. One such parameter is the assumed swimming speed of 6 cm s^{-1} that our simulated larvae reach after 1 yr. We have therefore repeated the calculations using a different speed (3 cm/s) in order to verify that the inter-annual variability is still significant and still originates largely from GS variability between 75W and 70W. These calculations are presented in Fig. S1 and described in Supporting Information.

Summary and conclusions

Our coupled bio-physical model of American eel larval dispersal suggests that natural oceanic variability can lead to changes in eel larval success rates by a factor of 2 (equivalent to a variation of 100%). Since all biological parameters were kept constant throughout all years in our numerical simulations, this variability is induced entirely by the open ocean circulation changes and applies to the larval phase of the eel life cycle only, without taking into account other factors that act during the same or other life stages. For this reason, comparison with available observational data on the YOY entrainment into estuaries or with commercial harvest time series have not been made. Even YOY abundance along the entire coast, which is arguably the closest observable to the larval success rates in reaching the shelf break, would depend strongly on many factors not included in our model. For example, Bonhommeau et al. (2008a,b) argue that glass eel recruitment is strongly affected by food availability during early larval stages. This availability is linked to primary productivity in the spawning area, which has a strong inverse relationship to water temperature in the Sargasso Sea. YOY abundance would also depend on the number of eggs laid in the Sargasso Sea, which depends on the number of successful adults reaching the spawning ground and, in turn, on the number of silver eels that undertook the migration and on the oceanic currents they encountered during the journey. This cause-and-effect sequence can be traced back from silver eel to YE and so on through the different life stages. Comparison with the YOY recruitment into rivers at specific locations is even more challenging due to the possible dependence on local precipitation, as documented by Sullivan et al. (2006). That said, our modeled range of larval success rate variability is in line with variability range in the commercial harvest of American Eel over the last decade (Casselman and Marcogliese 2007).

The larval success rates in the model are strongly affected by the GS inertial overshoot events, with the largest success in years with an inertial overshoot and the smallest in years with a straighter and more southern configuration of the GS downstream of Cape Hatteras. Because the overshoot events are characterized by a northward shift and an increase in the arclength of the jet centerline just downstream of Cape Hatteras, the mean GS length and latitude between 75W and 70W longitude can be used as proxies for characterizing the overshoot events. Both proxies were shown to correlate well with predicted larval success rates and thus could be converted into success rates using linear regression. This method works well, leading to a mean relative error of about 15% between the true and reconstructed success rates. Note that our two GS proxies are different from the Transport Index defined as the difference in potential energy anomalies between Bermuda and Labrador Basin that characterizes the intensity of the Gulf Stream and North Atlantic Current (Curry and McCartney 2001), and from the Gulf Stream Index that is a measure of the latitude of the Gulf Stream over a wide range of longitudes from 79W to 65W (Taylor and Stephens 1998). The Transport and Gulf Stream indices were previously examined by Bonhommeau et al. (2008b), who found no correlation between them and the European glass eel recruitment.

Model-based oceanic variability was compared to the observed variability of ocean currents based on AVISO satellite altimetry, and the two time series were shown to have comparable magnitudes of variability of the mean GS length and latitude, and the mean spectrum of one time series was shown to fall within the 1-std interval from the mean of the other. Assuming that the same relationship between overshoot events and the number of successful larvae reaching the 200 m isobath holds in the real ocean, AVISO-based mean GS length and latitude were converted into larval success rates, suggesting that the natural oceanic variability can cause inter-annual changes in larval success rates of about 75% of the time-mean value.

The significant inter-annual variability of larval success rates in our coupled physical–biological model and the

strong influence of the GS inertial overshoot events all point towards the general importance of the eddying component of the flow field in defining the larval success. Consistent with this expectation, the removal of the eddying component from the total FLAME-based velocities led to an approximately 3-fold drop in the resulting larval success rates, and to the increase of larval travel times to over 1 yr, which exceeds the biologically relevant duration of the larval stage. This suggests that eddies play a critical role in helping American eel larvae reach the coastal nursery habitats along the North American coast in a timely manner.

In this article, we have discovered a strong relationship between the state of the Gulf Stream and the success rates of American eel larvae. However, we have not investigated the physical mechanism underpinning this relationship; such an investigation is left for future study. Nevertheless, it is tempting to speculate on what physical processes could be responsible for the linkage between overshoot events and larval success rates. One simple, purely geometrical argument could be that during overshoot years the segment of the GS that runs parallel to the coast is longer, allowing eel larvae more time to detrain from the current on its shoreward side before it carries them too far off-shore. Alternative explanation might involve dynamics responsible for the weakening of the cross-jet barrier near the Gulf Stream core so that it becomes easier for the larvae to cross the jet during the overshoot years. These mechanisms, as well as others, are left for exploration in future studies.

References

ASMFC (Atlantic States Marine Fisheries Commission). 2012. American eel benchmark stock assessment. ASMFC Stock Assessment 12-01. Raleigh (NC): Atlantic States Marine Fisheries Commission [accessed 2013 March 20]. Available from http://www.asmfc.org/species/american-eel

ASMFC (Atlantic States Marine Fisheries Commission). 2014. Young of the Year (YOY) Update Analysis, American Eel Stock Assessment Subcommittee and Technical Committee. American Eel Board tasks to Technical Committee Memorandum. Available from http://www.asmfc.org/uploads/file/53b32b2fMay_2014_Eel_TC_Memo_Stock_Status.pdf

Atema, J., M. J. Kingsford, G. Gerlach, 2002. Larval reef fish could use odour for detection, retention and orientation to reefs. Marine Ecology Progress Series **241**, 151–160, doi:10.3354/meps241151

Biastoch, A., C. W. Böning, J. Getzlaff, J. -M. Molines, and G. Madec. 2008. Causes of interannual-decadal variability in the meridional overturning circulation of the midlatitude North Atlantic Ocean. J. Clim. **21**: 6599–6615. doi: 10.1175/2008JCLI2404.1

Bonhommeau, S., E. Chassot, B. Planque, E. Rivot, A. H. Knap, and O. Le Pape. 2008a. Impact of climate on eel populations of the Northern Hemisphere. Mar. Ecol. Prog. Ser. **373**: 71–80. doi:10.3354/meps07696

Bonhommeau, S., E. Chassot, and E. Rivot. 2008b. Fluctuations in European eel (Anguilla anguilla) recruitment resulting from environmental changes in the Sargasso Sea. Fish. Oceanogr. **17**: 32–44. doi:10.1111/j.1365-2419.2007.00453.x

Bonhommeau, S., and others. 2009. Estimates of the mortality and the duration of the trans-Atlantic migration of European eel Anguilla anguilla leptocephali using a particle tracking model. J. Fish Biol. **74**: 1891–1914. doi: 10.1111/j.1095-8649.2009.02298.x

Böning, C. W., M. Scheinert, J. Dengg, A. Biastoch, and A. Funk. 2006. Decadal variability of subpolar gyre transport and its reverberation in the North Atlantic overturning. Geophys. Res. Lett. **33**: L21S01. doi:10.1029/2006GL026906

Bower, A. S., and H. T. Rossby. 1989. Evidence of cross-frontal exchange processes in the Gulf Stream based on isopycnal RAFOS float data. J. Phys. Oceanogr. **19**: 1177–1190. doi: 10.1175/1520-0485(1989)019<1177:EOCFEP>2.0.CO;2

Bower, A. S., and M. S. Lozier. 1994. A closer look at particle exchange in the Gulf Stream. J. Phys. Oceanogr. **24**: 1399–1418. doi:10.1175/1520-0485(1994)024<1399:ACLAPE>2.0.CO;2

Brambilla, E., and L. D. Talley. 2006. Surface drifter exchange between the North Atlantic subtropical and subpolar gyres. J. Geophys. Res. **111**: C07026. doi:10.1029/2005JC003146

Burkholder, K. C., and M. S. Lozier. 2011. Subtropical to subpolar pathways in the North Atlantic: Deductions from Lagrangian trajectories. J. Geophys. Res. Oceans **116**: C07017. doi:10.1029/2010JC006697

Burkholder, K. C., and M. S. Lozier. 2014. Tracing the pathways of the upper limb of the North Atlantic Meridional Overturning Circulation. Geophys. Res. Lett. **41**: 4254–4260. doi:10.1002/2014GL060226

Casselman, J. M., and L. A. Marcogliese. 2007. Long-term changes in American eel (Anguilla rostrata) commercial harvest and price in relation to declining abundance. July 2007. MS report. Prepared for Great Lakes Fishery Commission, Ontario Ministry of Natural Resources, and Department of Fisheries and Oceans by AFishESci Inc., Bath, Ontario K0H 1G094 pp.

Castonguay, M., and J. D. McCleave. 1987. Vertical distributions, diel and ontogenetic vertical migrations and net avoidance of leptocephali of Anguilla and other common species in the Sargasso Sea. J. Plankton Res. **9**: 195–214. doi:10.1093/plankt/9.1.195

Castonguay, M., P. V. Hodson, C. Moriarty, K. F. Drinkwater, and B. M. Jessop. 1994. Is there a role of ocean environment in American and European eel decline? Fish. Oceanogr. **3**: 197–203. doi: 10.1111/j.1365-2419.1994.tb00097.x

Cowen, R. K., J. A. Hare, M. P. Fahay, 1993. Beyond hydrography: can physical processes explain larval fish assemblages within the Middle Atlantic Bight? Bulletin of Marine Science **53**, 567–587.

Curry, R. G., and M. S. McCartney. 2001. Ocean gyre circulation changes associated with the North Atlantic Oscillation. J. Phys. Ocranogr. **31**: 3374–3400. doi:10.1175/1520-0485(2001)031<3374:OGCCAW>2.0.CO;2

Dengg, J. 1993. The problem of Gulf Stream separation: A barotropic approach. J. Phys. Oceanogr. **23**: 2182–2200. doi: 10.1175/1520-0485(1993)023<2182:TPOGSS>2.0.CO;2

Dengg, J., A. Beckmann, and R. Gerdes. 1996. The Gulf Stream separation problem, p. 253–290. *In* W. Krauss [ed.], The Warmwatersphere of the North Atlantic Ocean. Gebr. Borntraeger.

Durif, C. M. F., H. I. Browman, J. B. Phillips, A. B. Skiftesvik, L. A. Vollestad, and H. H. Stockhausen. 2013. Magnetic compass orientation of the European eel. PLoS One **8**: e59212. doi:10.1371/journal.pone.0059212

Epifanio, C., 1995. Transport of blue crab (Callinectes sapidus) larvae in the waters off mid-Atlantic states. Bulletin of Marine Science **57**, 713–725, doi: 10/1995/57(3)713-725

Etherington, L. L., D. B. Eggleston, 2003. Spatial dynamics of large-scale, multistage crab (Callinectes sapidus) dispersal: determinants and consequences for recruitment. Canadian Journal of Fisheries and Aquatic Sciences **60**, 873–887, doi: 10.1139/F03-072

Fisher, R., D. R. Bellwood, and S. Job. 2000. Development of swimming abilities in reef fish larvae. Mar. Ecol. Prog. Ser. **202**: 163–173. doi:10.3354/meps202163

Fuglister, F. C. 1955. Alternate analyses of current surveys. Deep-Sea Res. **2**: 213–229. doi:10.1016/0146-6313(55)90026-5

Garvine, R., C. Epifanio, C. Epifanio, K. Wong, 1997. Transport and recruitment of blue crab larvae: a model with advection and mortality. Estuarine, Coastal and Shelf Science **45**, 99–111, doi:10.1006/ecss.1996.0161

Goodrich, D. M., J. van Montfrans, R. J. Orth, 1989. Blue crab megalopal influx to Chesapeake Bay: evidence for a wind-driven mechanism. Estuarine, Coastal and Shelf Science **29**, 247–260, doi:10.1016/0272-7714(89)90056-5

Govoni, J. J., H. L. Spach, 1999. Exchange and flux of larval fishes across the western Gulf Stream front south of Cape Hatteras, USA, in winter. Fisheries Oceanography **8**(Suppl. 2), 77–92, doi:10.1046/j.1365-2419.1

Gary, S. F., M. S. Lozier, Y. O. Kwon, and J. J. Park. 2014. The fate of North Atlantic subtropical mode water in the FLAME model. J. Phys. Oceanogr. **44**: 1354–1371. doi:10.1175/JPO-D-13-0202.1

Guillet, E. C. 1957. The valley of the Trent. Champlain Society.

Hare, J. A., J. H. Churchill, R. K. Cowen, T. J. Berger, P. C. Cornillon, P. Dragos, S. M. Glenn, J. J. Govoni, T. N. Lee, 2002. Routes and rates of larval fish transport from the southeast to the northeast United States continental shelf. Limnology and Oceanography **47**, 1774–1789, doi: 10.4319/lo.2002.47.6.1774

Hare, J. A., R. K. Cowen, 1996. Transport mechanisms of larval and pelagic juvenile bluefish (Pomatomus saltatrix) from South Atlantic Bight spawning grounds to Middle Atlantic Bight nursery habitats. Limnology and Oceanography **41**, 1264–1280, doi:10.4319/lo.1996.41.6.1264

Hare, J. A., J. A. Quinlan, F. E. Werner, B. O. Blanton, J. J. Govoni, R. B. Forward, L. R. Settle, D. E. Hoss, 1999. Larval transport during winter in the SABRE study area: results of a coupled vertical larval behaviour-three-dimensional circulation model. Fisheries Oceanography **8**(Suppl. 2), 57–76, doi:10.1046/j.1365-2419.1999.00017.x

Kleckner, R., and J. McCleave. 1985. Spatial and temporal distribution of American eel larvae in relation to North Atlantic Ocean current systems. Dana **4**: 67–92. URL: http://aims.fao.org/serials/c_4dc4e7ab

Kwon, Y. -O., J. J. Park, S. F. Gary, and M. S. Lozier. 2015. Year-to-year re-outcropping of Eighteen Degree Water in an eddy-resolving ocean simulation. J. Phys. Oceanogr. **45**: 1189–1204. doi:10.1175/JPO-D-14-0122.1

Lohmann, K. J., C. M. Lohmann, and N. F. Putman. 2007. Magnetic maps in animals: Nature's GPS. J. Exp. Biol. **210**: 3697–3705. doi:10.1242/jeb.001313

McCleave, J. 1993. Physical and behavioural controls on the oceanic distribution and migration of leptocephali. J. Fish Biol. **43**: 243–273. doi:10.1111/j.1095-8649.1993.tb01191.x

McCleave, J. D. 2008. Contrasts between spawning times of *Anguilla* species estimated from larval sampling at sea and from otolith analysis of recruiting glass eels. Mar. Biol. **155**: 249–262. doi:10.1007/s00227-008-1026-8

McCleave, J. D., R. C. Kleckner, and M. Castonguay. 1987. Reproductive sympatry of American and European eels and implications for migration and taxonomy, American Fisheries Society Symposium, pp. 286–297.

McCleave, J., P. J. Brickley, K. M. O'Brien, D. A. Kistner, M. W. Wong, M. Gallagher, and S. M. Watson. 1998. Do leptocephali of the European eel swim to reach continental waters? Status of the question. J. Mar. Biol. Assoc. UK **78**: 285–306. doi:10.1017/S0025315400040091

McGowan, M. F. and W. J. Richards, 1989. Bluefin Tuna, Thunnus thynnus, larvae in the Gulf Stream off the southeastern United States: satellite and shipboard observations of their environment. Fish. Bull. **87**, 615–631.

McMillen-Jackson, A. L., T. M. Bert, 2004. Mitochondrial DNA variation and population genetic structure of the blue crab Callinectes sapidus in the eastern United States. Marine Biology **145**, 769–777, doi:10.1007/s00227-004-1353-3

Miller, M. J. 2009. Ecology of anguilliform leptocephali: Remarkable transparent fish larvae of the ocean surface layer. Aqua-Bio Sci. Monogr. **2**: 1–94. doi:10.5047/absm.2009.00204.0001

Montgomery, J. C., A. Jeffs, S. D. Simpson, M. Meekan, C. Tindle, 2006. Sound as an orientation cue for the pelagic larvae of reef fishes and decapod crustaceans. Advances in Marine Biology **51**, 143–196, doi:10.1016/S0065-2881(06)51003-X

Morgan, L. H. 1877. Ancient society or researches in the lines of human progress from savagery through Barbarism to civilization. Henry Holt and Company. [Reprinted, 1963, World Publishing Company, Cleveland, and 1976, Gordon Press, New York.]

Mouritzen, H., J. Atema, M. J. Kingsford, and G. Gerlach. 2013. Sun compass orientation helps coral reef fish larvae return to their natal reef. PLoS One **8**: e66039. doi:10.1371/journal.pone.0066039

Özgökman, T. M., E. P. Chassignet, and A. M. Paiva. 1997. Impact of wind forcing, bottom topography, and inertia on midlatitude jet separation in a quasigeostrophic model. J. Phys. Oceanogr. **27**: 2460–2476. doi:10.1175/1520-0485(1997)027<2460:IOWFBT>2.0.CO;2

Pierini, S., P. Falco, G. Zambardino, T. A. McClimans, and I. Ellingsen. 2011. A laboratory study of nonlinear western boundary currents, with application to the Gulf Stream separation due to inertial overshooting. J. Phys. Oceanogr. **41**: 2063–2079. doi:10.1175/2011JPO4514.1

Quinlan, J. A., B. O. Blanton, T. J. Miller, F. E. Werner, 1999. From spawning grounds to the estuary: using linked individual-based and hydrodynamic models to interpret patterns and processes in the oceanic phase of Atlantic menhaden Brevoortia tyrannus life history. Fisheries Oceanography **8**(Suppl. 2), 224–246, doi:10.1046/j.1365-2419.1999.00033.x

Rypina, I. I., L. J. Pratt, and M. S. Lozier. 2011. Near-surface transport pathways in the North Atlantic Ocean: Looking for throughput from the subtropical to the subpolar gyre. J. Phys. Oceanogr. **41**: 911–925. doi:10.1175/201JPO4498.1

Righton, D., K. Aarestrup, D. Jellyman, P. Sebert, G. Van Den Thillart, and K. Tsukamoto, 2012. The Anguilla spp. migration problem: 40 million years of evolution and two millennia of speculation. J. Fish Biol., **81**: 365–386, doi: 10.1111/j.1095-8649.2012.03373.x

Rypina, I. I., J. K. Llopiz, L. J. Pratt, and M. S. Lozier. 2014. Dispersal pathways of American eel larvae from the Sargasso Sea. Limnol. Oceanogr. **59**: 1704–1714. doi:10.4319/lo.2014.59.5.1704

Schmidt, J. 1923. The breeding places of the eel. Phil. Trans. Roy. Soc. B **211**: 179–208. doi:10.1098/rstb.1923.0004

Schmidt, J. 1925. The breeding places of the eel. Ann. Rep. Smithsonian Inst. **1924**: 279–316. URL: http://www.jstor.org/stable/92087

Schmidt, J. 1931. Eels and conger eels of the North Atlantic. Nature **128**: 602–604. doi:10.1038/128602a0

Speck, F. G. 1939–1940. Miscellaneous notes, Scatticook, Two letters of Chief Swimming Eel to Speck, August 16, 1939 and August 5, 1940, concerning Indigenous social activities. American Philosophical Society Library [170(14: d90]. Available from http://www.amphilsoc.org/library/guides/indians/info/s.htm, File 3229.

Stegmann, P. M., J. A. Quinlan, F. E. Werner, B. O. Blanton, P. Berrien, 1999. Atlantic menhaden recruitment to a southern estuary: defining potential spawning regions. Fisheries Oceanography **8**(Suppl. 2), 111–123, doi: 10.1046/j.1365-2419.1999.00022.x

Sullivan, M., K. Able, J. Hare, H. Walsh, 2006. Anguilla rostrata glass eel ingress into two, US east coast estuaries: patterns, processes and implications for adult abundance. Journal of Fish Biology, **69**, 1081–1101, doi:10.1111/j.1095-8649.2006.01182.x

Taylor, A. H., and J. A. Stephens. 1998. The North Atlantic Oscillation and the latitude of the Gulf Stream. Tellus **50A**: 134–142. doi:10.1034/j.1600-0870.1998.00010.x

Tilburg, C. E., A. I. Dittel, C. E. Epifanio, 2007. Retention of crab larvae in a coastal null zone. Estuarine, Coastal, and Shelf Science **72**, 570–578, doi:10.1016/j.ecss.2006.11.030

Tooker, E. 1978. The league of the Iroquois: Its history, politics, and ritual, p. 418–441. *In* Handbook of North American Indians 15. Smithsonian Institution.

Werner, F. E., B. O. Blanton, J. A. Quinlan, R. A. Luettich Jr, , 1999. Physical oceanography of the North Carolina continental shelf during the fall and winter seasons: implications for the transport of larval menhaden. Fisheries Oceanography **8**(Suppl. 2), 7–21, doi:10.1046/j.1365-2419.1999.00016.x

Wiltschko, R., and W. Wiltschko. 1995. Magnetic orientation in animals. Springer.

Wuenschel, M., and K. Able. 2008. Swimming ability of eels (*Anguilla rostrata, Conger oceanicus*) at estuarine ingress: contrasting patterns of cross-shelf transport? Mar. Biol. **154**: 775–786. doi:10.1007/s00227-008-0970-7

Zhang, R., and J. K. Vallis. 2007. The role of bottom vortex stretching on the path of the North Atlantic Western boundary current and on the northern recirculation gyre. J. Phys. Oceanogr. **37**: 2053–2080. doi:10.1175/JPO3102.1

Acknowledgments

I.I.R. and L.J.P. were supported by grant 85464100 (OCE-1154641) from the National Science Foundation. M.S.L. gratefully acknowledges support from the National Science Foundation.

Submitted 21 September 2015
Revised 24 December 2015
Accepted 1 March 2016

Associate editor: Bernadette Sloyan